6710 J. Am. Chem. Soc. 1993, 115, 6710–6717

Stability of Vanadium(II) Aryloxides: Synthesis and Characterization of Sterically Protected, Neutral and Monomeric Vanadium(II) Aryloxides. Reactivity with the N–N Bond of $(Me_3Si)CH{=}N{=}N$

Ravinder K. Minhas,[†] **Jilles J. H. Edema,**[†] **Sandro Gambarotta,**[*,†] **and Auke Meetsma**[‡]

Contribution from the Departments of Chemistry, University of Ottawa, Ottawa, Ontario K1N 6N5, Canada, and Rijksuniversiteit Groningen, Groningen 9747 AG, The Netherlands

Received December 14, 1992

Abstract: The preparation of neutral V(II) aryloxides has been achieved via ligand-replacement reactions on three V(II) complexes $(Mz_2V(py))_2(\mu\text{-}N_2)$, $Mz_2V(py)_2$, and $VCl_2(TMEDA)_2$ (Mz = $o\text{-}Me_2NCH_2C_6H_4$, TMEDA = *N,N,N′,N′*-tetramethylethylenediamine) with several phenols, or their corresponding alkali salts. In the case of sterically demanding phenols [2,6-(*t*-Bu)$_2$-4-MeC_6H_2OH, 2,6-Ph_2PhOH, 2-(MeO)C_6H_4OH] it was possible to isolate and characterize monomeric and neutral V(II) aryloxides with a variety of coordination geometries. When similar reactions were carried out on the same complexes with less bulky alcohols (2,6-Me_2PhOH, PhOH, *t*-BuOH), monomeric V(III) and dimeric V(III)/V(IV) mixed-valence species were isolated. The crystal structures of the square-planar [2,6-(*t*-Bu)$_2$-4-$MeC_6H_2O]_2V(py)_2$ (**4**), saddle-shape (2,6-$Ph_2PhO)_2V$(TMEDA) (**5**), square-pyramidal (2,6-$Ph_2PhO)_2V(py)_3$ (**6**), and octahedral [2-(MeO)$C_6H_4O]_2V$(TMEDA) (**7**) were demonstrated by X-ray diffraction analysis. Crystal data are as follows. **4**: $C_{40}H_{56}VN_2O_2{\cdot}(C_7H_8)_2$, M_r = 833.12, triclinic, $P\bar{1}$, a = 9.701(2) Å, b = 15.303(3) Å, c = 9.000(2) Å, α = 101.99(2)°, β = 112.59(2)°, γ = 74.20(2)°, V = 1179.0(4) Å^3, Z = 1, λ = 0.710 69 Å, R = 0.053, R_w = 0.068, and GoF = 2.89 for 365 parameters and 3475 out of 4134 unique reflections. **5**: $C_{42}H_{42}N_2O_2V$, M_r = 657.74, monoclinic, $P2_1/a$, a = 16.373(1) Å, b = 11.1624(9) Å, c = 19.536(3) Å, β = 97.35(1)°, V = 3541.3(7) Å^3, Z = 4, λ = 0.709 30 Å, R = 0.044, R_w = 0.017, and GoF = 1.63 for 589 parameters and 2714 out of 4603 unique reflections. **6**: $C_{51}H_{41}N_3O_2V$, M_r = 778.85, monoclinic, $C2/c$, a = 20.65(2) Å, b = 14.28(1) Å, c = 16.08(1) Å, β = 119.89(7)°, V = 4113.(7) Å^3, Z = 4, R = 0.053, R_w = 0.049, and GoF = 1.34 for 259 parameters and 1505 out of 3182 unique reflections. **7**: $C_{20}H_{30}VN_2O_4$, M_r = 413.41, orthorhombic, $Pna2_1$, a = 13.519(5) Å, b = 13.846(4) Å, c = 11.196(2) Å, V = 2096(1) Å^3, Z = 4, R = 0.037, R_w = 0.047, and GoF = 1.96 for 244 parameters and 1669 out of 2116 unique reflections. Reaction of **7** with $(Me_3Si)CHN_2$ gave the new diamagnetic and dinuclear complex {[2-(MeO)$C_6H_4O]_2V\}_2[\mu$-NNCH-$(SiMe_3)]_2$ (**13**). Complex **13** was co-crystallized in a 1/1 ratio with {[2-(MeO)$C_6H_4O]_2V\}_2[\mu\text{-}OC_6H_4(2\text{-}OCH_3)]_2$, which was formed from the thermal degradation of **13** through a complicated reaction. Crystal data for the co-crystallite {[2-MeO)$C_6H_4O]_2V\}_2[\mu\text{-}NNCH(SiMe_3)]_2$/{[2-MeO)$C_6H_4O]_2V\}_2[\mu\text{-}OC_6H_4(2\text{-}OCH_3)]_2$ (**14**) are as follows. **14**: $C_{39}H_{45}V_2N_2O_{10}Si$, M_r = 831.76, triclinic, $P\bar{1}$, a = 14.443(6) Å, b = 15.039(6) Å, c = 10.679(3) Å, α = 100.66(3)°, β = 97.46(3)°, γ = 113.84(3)°, V = 2030(1) Å^3, Z = 2, R = 0.045, R_w = 0.060, and GoF = 2.45 for 488 parameters and 5530 out of 6946 unique reflections.

Introduction

Disproportionation or electron-transfer reactions are among the most common reaction pathways through which a transition metal complex, in unstable oxidation state, decomposes. The most obvious strategy for preventing unwanted easy disproportionations, which are occasionally a severe obstacle to synthetic efforts, is to bury the transition metal inside large and inert organic matrices of bulky ligands, thereby leaving little possibility for the transition metal to reorganize the molecule and modify the oxidation state. This strategy, which is suggested by the performances of transition metals in bioinorganic systems, has been successfully used in a number of cases and, in the chemistry of early transition metals, has allowed the isolation of transition metals in unstable oxidation states,[1] or in unusual coordination geometries,[2] and the trapping and stabilization of many diverse highly-reactive functionalities.[3]

The poor development of the coordination chemistry of divalent vanadium and in particular of its alkoxide derivatives can be ascribed to the instability of this oxidation state. For example, simple V(II) aryloxides are extremely rare[4] despite the strong interest stimulated by the initial discovery that a few cycles of catalytic transformation of dinitrogen into NH_3 and hydrazine are promoted by *in situ* generated V(II) catecholate or hydroxide, just before irreversible oxidation of the metal center takes place.[5] This suggests that V(II) species supported by oxygen-containing ligands might be very promising starting materials for reactivity studies and therefore encourages further synthetic efforts to prevent oxidation or disproportionation. Interest in the chemistry of V(II) alkoxides has been also stimulated by the fact that these species may conveniently serve as starting materials for the preparation of high-nuclearity oxo/alkoxovanadates, which have recently been shown to play a relevant role in some important biological processes.[6] The synthetic difficulties generally encountered in the preparation of V(II) complexes seem to be caused by an apparent instability of the divalent state with respect to

---

[†] University of Ottawa.

[‡] Rijksuniversiteit Groningen.

(1) (a) Hitchcock, P. B.; Lappert, M. F.; Lawless, G. A.; Olivier, H.; Ryan, E. J. *J. Chem. Soc., Chem. Commun.* **1992**, 474. (b) Urazowski, I. F.; Ponomaryev, V. I.; Nifant'ev, I. E.; Leminovskii, D. A. *J. Organomet. Chem.* **1989**, *368*, 287. (c) Evans, W. J.; Grate, J. W.; Doedens, R. J. *J. Am. Chem. Soc.* **1985**, *107*, 1671. (d) Durfee, L. D.; Fanwick, P. E.; Rothwell, I. P.; Folting, K.; Huffman, J. C. *J. Am. Chem. Soc.* **1987**, *109*, 4720. (e) Gambarotta, S.; Chiang, M. *J. Chem. Soc., Chem. Commun.* **1987**, 698.

(2) (a) LaDuca, R. L.; Wolczanski, P. T. *Inorg. Chem.* **1992**, *31*, 1311. (b) Covert, K. J.; Neithamer, D. R.; Zonnevylle, M. C.; LaPointe, R. E.; Schaller, C. P.; Wolczanski, P. T. *Inorg. Chem.* **1991**, *30*, 2494. (c) Evans, W. J.; Drummond, D. K.; Zhang, H.; Atwood, J. L. *Inorg. Chem.* **1988**, *27*, 575. (d) Edema, J.; Gambarotta, S.; Spek, A. L. *Inorg. Chem.* **1989**, *28*, 811.

0002-7863/93/1515-6710$04.00/0

either disproportionation toward higher and lower oxidation states or deoxygenation reactions.[7] Attempts to prepare metal V(II) aryloxides via mild-condition ligand replacement on V(II) starting compounds have also been unsuccessful,[8] only two V(II) anionic aryloxides having been reported so far.[4]

In this work, we report the synthesis and characterization of the first series of neutral V(II) aryloxides stabilized by sterically demanding or chelating aryloxides. In an attempt to gain insight into their ability to interact with dinitrogen, we have also carried out mild-condition ligand replacement reactions on a preformed V–(N_2)–V frame of an aryl–dinitrogen–vanadium complex $[Mz_2Vpy]_2(\mu\text{-}N_2)$ [Mz = $o\text{-}Me_2NCH_2C_6H_4$].[9] We now describe the reaction of this dinitrogen compound and of other V(II) compounds with a series of phenols and corresponding alkali salts together with a preliminary study on the reactivity with the N–N multiple bond of a diazoalkane.

Experimental Section

All operations were performed under an inert atmosphere in a nitrogen-filled drybox (Vacuum Atmosphere) or by using standard Schlenk techniques. $[Mz_2V(py)]_2(N_2)(thf)_2$ (**1**),[9] $Mz_2V(py)_2$ (**2**),[10] *trans*-$(TMEDA)_2VCl_2$ (**3**),[10] $Mes_3V(THF)$,[11] and $\{[2,6\text{-}(MeO)_2C_6H_3]_2V\}_2(THF)$[12] [TMEDA = *N,N,N′,N′*-tetramethylethylenediamine; Mz = $2\text{-}Me_2NCH_2C_6H_4$; Mes = $2,4,6\text{-}Me_3C_6H_2$; py = pyridine] were prepared according to published procedures. TMEDA was chromatographed over Al_2O_3 and distilled over molten potassium after reflux; pyridine was refluxed over CaH_2 and distilled under nitrogen using a Vigreux column. Phenols (Aldrich) were sublimed before use. NaH (suspension in mineral oil) was washed with hexane, dried, and stored under nitrogen in sealed ampules. Infrared spectra were recorded on a Perkin-Elmer 283 instrument from Nujol mulls prepared in a drybox. Samples for magnetic susceptibility measurements of complex **4** were weighed inside a drybox equipped with a microanalytical balance, and sealed into a specially designed Teflon capsule. Data were recorded at variable temperatures in the range 100–298 K by using a Faraday balance (Oxford Instruments) interfaced with an Apple II Computer. Plots of $1/\chi_g$ against T (K) were in satisfactory agreement with the Curie–Weiss law. The magnetic moment was calculated by following standard methods,[13] and corrections for underlying diamagnetism were applied to the data.[14] Magnetic measurements of all the other complexes were carried out with a Gouy balance (Johnson Matthey) at room temperature on sealed tubes of samples prepared in the drybox.

$\{[2,6\text{-}(t\text{-}Bu)_2\text{-}4\text{-}Me\text{-}C_6H_2O]_2V(py)_2\}\cdot 2C_7H_8$ (4). Method A. A solution of $[Mz_2V(py)]_2(\mu\text{-}N_2)(THF)_2$ (1.3 g, 1.4 mmol) in THF (20 mL) was stirred with $2,6\text{-}(t\text{-}Bu)_2\text{-}4\text{-}Me\text{-}C_6H_2OH$ (1.2 g, 5.6 mmol). The solution turned deep orange, and stirring was continued for 3 h. After solvent evaporation *in vacuo*, the residual solid was recrystallized from pentane (50 mL). Brown-red crystals of **4** were obtained upon standing at −30 °C overnight (yield 0.73 g, 0.9 mmol, 32%). Anal. Calcd (found) for $C_{54}H_{72}VN_2O_2$: C, 77.94 (77.88); H, 8.72 (8.44); N, 3.37 (3.07); V, 6.12 (5.89). IR [Nujol, KBr, cm^{-1}]: 1600 (s), 1410 (m), 1350 (m), 1260 (s), 1210 (m), 1195 (w), 1155 (w), 1020 (w), 880 (m), 860 (s), 835 (s), 805 (m), 780 (m), 765 (s), 720 (w), 705 (s), 655 (w), 620 (w). μ_{eff} = 3.71 μ_B.

Method B. A toluene solution (50 mL) of **2** (1.0 g, 1.7 mmol) was treated with neat $2,6\text{-}(t\text{-}Bu)_2\text{-}4\text{-}Me\text{-}C_6H_2OH$ (0.7 g, 3.3 mmol). The emerald green color turned suddenly deep orange. Brown-red crystals of **4** (0.5 g, 0.6 mmol, 35%) were isolated after concentration to small volume and layering with hexane.

Method C. A THF solution (50 mL) of $2,6\text{-}(t\text{-}Bu)_2\text{-}4\text{-}Me\text{-}C_6H_2ONa$, prepared *in situ* by treating the corresponding phenol (4.6 g, 20.9 mmol) with NaH (0.8 g, 33 mmol), was reacted with $VCl_2(TMEDA)_2$ (3.7 g, 10.4 mmol). Further addition of pyridine (1.7 g, 21 mmol) changed the color from green to red-brown. The resulting mixture was boiled and the reflux continued overnight. After filtration and concentration, the solvent was removed *in vacuo* and the residual solid redissolved in toluene (50 mL). Brown-red crystals of **4** (5.2 g, 6.2 mmol, 60%) were separated after the solution was layered with hexane and allowed to stand overnight at room temperature.

$(2,6\text{-}Ph_2PhO)_2V(TMEDA)$ (5). A solution of 2,6-diphenylphenol (2.5 g, 10 mmol) in THF (75 mL) was stirred and boiled overnight with NaH (0.4 g, 16 mmol). The addition of solid $VCl_2(TMEDA)_2$ (1.8 g, 5.0 mmol) turned the color red. The mixture was stirred for 1 h and filtered, and the solvent was removed *in vacuo*. The solid residue was redissolved in toluene (30 mL), and hexane (60 mL) was added to the resulting solution. Large red crystals of **5** (2.5 g, 3.8 mmol, 76%) separated upon standing overnight at −30 °C. Anal. Calcd (found) for $C_{42}H_{42}O_2N_2V$: C, 76.69 (76.55); H, 6.44 (6.31); N, 4.26 (4.32); V, 7.74 (7.12). IR [Nujol, KBr, cm^{-1}]: 1580 (s), 1550 (m), 1450 (s), 1420 (s), 1405 (w), 1350 (w), 1300 (s), 1280 (m), 1245 (s), 1175 (w), 1120 (w), 1110 (w), 1075 (w), 1060 (m), 1040 (w), 1005 (m), 995 (w), 950 (s), 930 (w), 915 (w), 860 (s), 800 (s), 750 (s), 740 (s), 725 (m), 710 (w), 700 (s), 600 (s), 585 (s), 550 (m), 510 (m), 500 (m). μ_{eff}(291 K) = 3.63 μ_B.

$(2,6\text{-}Ph_2PhO)_2V(py)_3$ (6). Method A. Treatment of a THF solution (25 mL) of **5** (1.6 g, 2.4 mmol) with pyridine (2 mL) yielded large deep red crystals of **6** (1.1 g, 1.4 mmol, 58%). Anal. Calcd (found) for

---

(3) For example, hydrides: (a) Wolczanski, P.; Bercaw, J. E. *Organometallics* **1982**, *1*, 793 and references cited therein. (b) Choukroun, R.; Dahan, F.; Larsonneur, A.; Samuel, E.; Petersen, J.; Meunier, P.; Sornay, C. *Organometallics* **1991**, *10*, 374. Acyls: Campion, B. K.; Falk, J.; Tilley, T. D. *J. Am. Chem. Soc.* **1987**, *109*, 2049 and references cited therein. Ketenes: (c) Martin, B. D.; Matchett, S. A.; Norton, J. R.; Anderson, O. P. *J. Am. Chem. Soc.* **1985**, *107*, 7952. (d) Waymouth, R. M.; Santarsiero, B. D.; Coots, R. J.; Bronikowski, M. J.; Grubbs, R. H. *J. Am. Chem. Soc.* **1986**, *108*, 1427. Olefins: (e) Fisher, R. A.; Buchwald, S. L. *Organometallics* **1990**, *9*, 871. (f) Cohen, S. A.; Bercaw, J. E. *Organometallics* **1985**, *4*, 1006. (g) Cohen, S. A.; Auburn, P. R.; Bercaw, J. E. *J. Am. Chem. Soc.* **1983**, *105*, 1136. (h) Hill, J. E.; Fanwick, P. E.; Rothwell, I. P. *Organometallics* **1992**, *11*, 1771 and references cited therein. (i) Fryzuk, M. D.; Haddad, T. S.; Rettig, S. J. *Organometallics* **1988**, *7*, 1224. (j) Roddick, D. M.; Fryzuk, M. D.; Seidler, P. F.; Hillhouse, G. L.; Bercaw, J. E. *Organometallics* **1985**, *4*, 97. Alkynes: (k) Buchwald, S. L.; Watson, B. T.; Huffman, J. C. *J. Am. Chem. Soc.* **1986**, *108*, 7411 and references cited therein. (l) Erker, G.; Czisch, P.; Mynott, R. *Z. Naturforsch.* **1985**, *40b*, 1177. Imides: (m) Walsh, P. J.; Hollander, F. J.; Bergman, R. G. *J. Am. Chem. Soc.* **1990**, *112*, 894. (n) Cummins, C.C.; Baxter, S. M.; Wolczanski, P. T. *J. Am. Chem. Soc.* **1988**, *110*, 8731 and references cited therein. (o) Hill, J. E.; Profilet, R. D.; Fanwick, P. E.; Rothwell, I. P. *Angew. Chem., Int. Ed. Engl.* **1990**, *29*, 664. (p) Bradley, D. C.; Errington, R. J.; Hursthouse, M. B.; Short, R. L.; Ashcroft, B. R.; Clark, G. R.; Nielson, A. J.; Rickard, C. E. F. *J. Chem. Soc., Dalton Trans.* **1987**, 2067 and references cited therein. Dinitrogen: (q) Sanner, R. D.; Manriquez, J. M.; Marsch, R. E.; Bercaw, J. E. *J. Am. Chem. Soc.* **1976**, *98*, 8351. (r) Fryzuk, M. D.; Haddad, T. S.; Rettig, S. J. *J. Am. Chem. Soc.* **1990**, *112*, 8185. (s) Duchateau, R.; Gambarotta, S.; Beydoun, N.; Bensimon, C. *J. Am. Chem. Soc.* **1991**, *113*, 8986. (t) Churchill, M. R.; Li, Y. J.; Theopold, K. H.; Schrock, R. R. *Inorg. Chem.* **1984**, *23*, 4472. Carbene: (u) Aguero, A.; Kress, J.; Osborn, J. A. *J. Chem. Soc., Chem. Commun.* **1985**, 793. (v) Liu, A. H.; Murray, R. C.; Dewan, J. C.; Santarsiero, B. D.; Schrock, R. R. *J. Am. Chem. Soc.* **1987**, *109*, 4282. (w) Chisholm, M. H.; Heppert, J. A.; Kober, E. M.; Lichtenberger, D. L. *Organometallics* **1987**, *6*, 1065. Dihydrogen: Wasserman, H. J.; Kubas, G. J.; Ryan, R. R. *J. Am. Chem. Soc.* **1986**, *108*, 2294 and references cited therein. Carbon dioxide: Fu, P.; Khan, M. A.; Nicholas, K. M. *Organometallics* **1992**, *11*, 2607.

(4) (a) Scott, M. J.; Wilisch, W. C. A.; Armstrong, W. H. *J. Am. Chem. Soc.* **1990**, *112*, 2429. (b) Floriani, C.; Mazzanti, M.; Chiesi-Villa, A.; Guastini, C. *Angew. Chem., Int. Ed. Engl.* **1988**, *27*, 576.

(5) (a) Denisov, N. T.; Efimov, O. N.; Shuvalova, N. I.; Shilova, A. K.; Shilov, A. E. *Zh. Fiz. Khim.* **1970**, *44*, 2694. (b) Shilov, A. E.; Denisov, N. T.; Efimov, O. N.; Shuvalov, N. F.; Shuvalova, N. I.; Shilova, E. *Nature (London)* **1971**, *231*, 460. (c) Zones, S. I.; Vickrey, T. M.; Palmer, J. G.; Schrauzer, G. N. *J. Am. Chem. Soc.* **1976**, *98*, 7289. (d) Zones, S. I.; Palmer, M. R.; Palmer, J. G.; Doemeny, J. M.; Schrauzer, G. N. *J. Am. Chem. Soc.* **1978**, *100*, 2113. (e) Schrauzer, G. N.; Strampach, N.; Hughes, L. A. *Inorg. Chem.* **1982**, *21*, 2184. (f) Luneva, N. P.; Moravsky, A. P.; Shilov, A. E. *Nouv. J. Chim.* **1982**, *6*, 245. (g) Luneva, N. P.; Nikonova, L. A.; Shilov, A. E. *Kinet. Katal.* **1977**, *18*, 212. (h) Schrauzer, G. N., Palmer, M. R. *J. Am. Chem. Soc.* **1981**, *103*, 2659. (i) Yamamoto, A.; Go, S.; Ookawa, M.; Takahashi, M.; Ikeda, S.; Keii, T. *Bull. Chem. Soc. Jpn.* **1972**, *45*, 3110. (j) Henderson, R. A.; Leigh, G. J.; Pickett, C. J. *Adv. Inorg. Chem. Radiochem.* **1983**, *27*, 197.

(6) (a) Crans, D. C.; Felty, R. A.; Miller, M. M. *J. Am. Chem. Soc.* **1991**, *113*, 265. (b) Crans, D. C.; Rithner, C. D.; Theisen, L. A. *J. Am. Chem. Soc.* **1990**, *112*, 2901.

(7) See for example: Cotton, F. A.; Extine, M. W.; Falvello, L. R.; Lewis, D. B.; Lewis, G. E.; Murillo, C. A.; Schwotzer, W.; Tomas, M.; Troup, J. M. *Inorg. Chem.* **1986**, *25*, 3505.

(8) (a) Gambarotta, S.; vanBolhuis, F.; Chiang, M. Y. *Inorg. Chem.* **1987**, *26*, 4301. (b) Wilisch, W. C. A.; Scott, M. J.; Armstrong, W. H. *Inorg. Chem.* **1988**, *27*, 4333.

(9) Edema, J. J. H.; Meetsma, A.; Gambarotta, S. *J. Am. Chem. Soc.* **1989**, *111*, 6878.

(10) Edema, J. J. H.; Stauthamer, W.; Van Bolhuis, F.; Gambarotta, S.; Smeets, W. J.; Spek, A. L. *Inorg. Chem.* **1990**, *29*, 1302.

(11) Seidel, W.; Kreisel, G. *Z. Anorg. Allg. Chem.* **1977**, *435*, 146.

(12) Seidel, W.; Kreisel, G., Mennega, H. *Z. Chem.* **1976**, *16*, 492.

(13) Mabbs, M. B.; Machin, D. J. *Magnetism and Transition Metal Complexes*; Chapman and Hall: London, 1973.

(14) Foese, G.; Gorter, C. J.; Smits, L. J. *Selected Diamagnetic, Paramagnetic, and Paramagnetic Relaxation Constants*; Masson: Paris, 1957.

$C_{51}H_{41}O_2N_3V$: C, 78.65 (78.33); H, 5.31 (5.29); N, 5.40 (5.18); V, 6.54 (6.33). IR [Nujol, KBr, cm^{-1}]: 1580 (s), 1495 (s), 1420 (m), 1380 (s), 1300 (m), 1260 (m), 1205 (m), 1180 (w), 1150 (w), 1065 (w), 1045 (w), 1010 (w), 980 (w), 940 (w), 800 (s), 760 (s), 750 (m), 735 (s), 700 (s), 600 (m), 505 (m). μ_{eff}(291 K) = 3.72 μ_B.

Method B. An emerald-green solution of **2** (1.0 g, 1.7 mmol) in toluene (50 mL) was treated with 1 equiv of pyridine and neat Ph_2PhOH (0.8 g, 3.3 mmol). The color turned deep brown, and large deep red crystals of **6** separated upon standing overnight at -30 °C.

Method C. The above procedure was followed but using **1** (1.5 g, 1.6 mmol) as starting material. Deep red crystals of **6** were isolated in poor yield (11%).

[2-(OCH$_3$)C$_6$H$_4$O]$_2$V(TMEDA) (7). Method A. A solution of guaiacol (3.3 g, 27 mmol) in THF (70 mL) was stirred and refluxed over NaH (1.0 g, 40 mmol). The excess NaH was filtered out and the resulting solution treated with $VCl_2(TMEDA)_2$ (4.8 g, 13.5 mmol). The resulting green solution was stirred for 3 h. After evaporation to dryness and addition of toluene (50 mL), the mixture was filtered and layered with ether (20 mL). Brown-orange crytals of **7** (2.8 g, 6.8 mmol, 52%) separated upon standing 1 day at room temperature. Anal. Calcd (found) for $C_{20}H_{30}O_4N_2V$: C, 58.11 (58.03); H, 7.31 (7.29); N, 6.78 (6.38); V, 12.32 (12.23). IR [Nujol, KBr, cm^{-1}]: 1590 (s), 1460 (s), 1325 (s), 1300 (s), 1250 (m), 1200 (s), 1160 (s), 1110 (m), 1060 (w), 1020 (s), 950 (w), 930 (w), 900 (w), 850 (m), 840 (w), 830 (w), 800 (m), 745 (s), 730 (m), 595 (m), 430 (m). μ_{eff}(291 K) = 3.83 μ_B.

Method B. A light blue solution of $VCl_2(TMEDA)_2$ (1.9 g, 5.3 mmol) in THF (100 mL) was reacted with neat guaiacol (1.3 g, 11 mmol) in the presence of small excess of TMEDA (1.7 g, 14 mmol). The color turned suddenly orange. The mixture was boiled and evaporated to dryness. The residual solid was suspended in toluene, the insoluble solid filtered off, and the filtrate layered with ether. Brown-orange crystals of **7** (1.3 g, 3.1 mmol, 58%) separated upon standing overnight at room temperature.

(Guac)$_2$V(py)$_2$ (8). The addition of pyridine (1.5 mL) to a deep green-yellow toluene solution (40 mL) of **7** (0.8 g, 1.9 mmol) turned the color violet. The solution was concentrated to small volume and layered with hexane. Violet microcrystalline **8** (0.3 g, 0.6 mmol, 34%) was obtained upon standing overnight at room temperature. Anal. Calcd (found) for $C_{24}H_{24}O_4N_2V$: C, 63.30 (63.01); H, 5.31 (5.11); N, 6.15 (6.00); V, 11.19 (11.07). IR [Nujol, KBr, cm^{-1}]: 1570 (m), 1430 (m), 1310 (sh), 1290 (m), 1260 (sh), 1240 (sh), 1195 (sh), 1155 (sh), 1090 (sh), 1010 (w), 840 (m), 830 (m), 730 (w), 675 (sh), 575 (m), 400 (w). μ_{eff}(291 K) = 3.53 μ_B.

(2,6-Me$_2$C$_6$H$_3$O)$_3$V(Py)$_2$ (10). The addition of neat $2,6\text{-}Me_2C_6H_3$-OH (0.85 g, 4.0 mmol) to a deep-green solution of **2** (1.0 g, 2.0 mmol) in toluene (50 mL) turned the color deep-orange. The solution was concentrated to small volume. Bright-orange crystals of **10**[8a] separated upon standing at low temperature overnight (0.3 g, 0.5 mmol, 25%).

[(t-BuO)$_2$V]$_2$(μ-t-BuO)(μ-O) (11). Method A. The addition of freshly distilled t-BuOH (0.65 g, 8.7 mmol) to a solution of $Mes_3V(THF)$ (1.4 g, 2.9 mmol) in toluene (100 mL) turned the color intensely purple. The solvent was removed *in vacuo* and the oily residue sublimed *in vacuo* (2 mmHg, 120–150 °C), yielding deep purple crystals of **11** (0.54 g, 1.1 mmol, 69%). Anal. Calcd (found) for $C_{20}H_{45}O_6V_2$: C, 49.69 (49.27); H, 9.38 (9.01); V, 21.07 (20.81). IR [Nujol, KBr, cm^{-1}]: 2940 (s), 2900 (s), 2830 (s), 1560 (w), 1445 (s), 1382 (s), 1351 (s), 1239 (w), 1216 (m), 1175 (s), 1090 (w), 980 (s), 930 (w), 894 (m), 825 (w), 795 (m), 778 (s), 761 (s), 719 (w), 649 (s), 590 (s), 492 (m), 472 (w), 401 (w). μ_{eff}(291 K) = 2.71 μ_B.

Method B. The same procedure as above was followed using $\{[2,6\text{-}(MeO)_2C_6H_3]_2V\}_2(THF)_2$ (1.0 g, 1.2 mmol) as starting material. Yield: 0.12 g, 0.25 mmol, 20%.

(C$_6$H$_5$O)$_3$V(TMEDA) (12). A solution of C_6H_5OH (1.7 g, 18 mmol) in THF (70 mL) was boiled overnight over NaH (0.64 g, 26 mmol). The excess NaH was filtered off, and $VCl_2(TMEDA)_2$ (3.2 g, 9.0 mmol) was added to the solution. The color turned greenish-orange, and stirring was continued for 2 h. After evaporation of the solvent in vacuo the residual solid was redissolved in toluene and the residual solution was layered with hexane after filtration. Green crystals of **12** (2.2 g, 4.9 mmol, 54%) separated upon standing at -30 °C overnight. Anal. Calcd (found) for $C_{24}H_{31}O_3N_2V$: C, 64.57 (63.12); H, 7.00 (7.12); V, 12.57 (12.21). IR [Nujol, KBr, cm^{-1}]: 1580 (sh), 1318 (m), 1330 (m), 1260 (br), 1190 (w), 1160 (sh), 1120 (w), 1065 (m), 1040 (w), 1020 (sh), 990 (sh), 955 (sh), 890 (br), 850 (w), 830 (sh), 800 (sh), 760 (sh), 725 (m), 695 (sh), 575 (sh), 520 (w). μ_{eff}(291 K) = 2.78 μ_B.

{[2-(CH$_3$O)C$_6$H$_4$]$_2$V}$_2$[μ-NN=CH(SiMe$_3$)]$_2$·toluene (13). A solution of **7** (1.2 g, 3.0 mmol) in toluene (40 mL) was treated with $(Me_3Si)CHN_2$ (1.48 mL, 3.0 mmol). The initial greenish-orange color slowly turned reddish-brown. After stirring 24 h at room temperature, the resulting deep reddish-orange solution was layered with hexane and allowed to stand overnight at room temperature. Black microcrystals of **13** (0.6 g, 0.7 mmol, 46%) separated. Anal. Calcd (found) for $C_{36}H_{36}O_8N_4V_2Si_2$: C, 53.33 (53.12); H, 4.48 (4.01); V, 12.57 (12.13). ^1H NMR (200 MHz, benzene-d_6, 26 °C, δ): 7.40 (s, 1H, C–H diazo), 7.10 (m, toluene and C_6D_6), 7.02 (m, toluene), 6.83 (m, 4H, guaiacol), 6.52 (pseudot, 2H, guaiacol), 6.36 (pseudot, 2H, guaiacol), 3.77 (s, 6H, guaiacol), 2.10 (s, 3 H, toluene), –0.05 (s, 9H, Me_3Si).

{[2-(CH$_3$O)C$_6$H$_4$]$_2$V}$_2$[(μ-NNCH(SiMe$_3$)]$_2$/{[2-(CH$_3$O)C$_6$H$_4$]$_2$V}$_2$[μ-2-(CH$_3$O)C$_6$H$_4$]$_2$ (14). A toluene solution of **13**, prepared as above and by using similar amounts, was boiled for a few minutes and then worked up in the usual manner. Dark-orange crystals of the co-crystallite separated upon standing overnight at room temperature (24%). IR [Nujol, KBr, cm^{-1}]: 1595 (w), 1360 (m), 1310 (m), 1300 (s), 1265 (sh), 1235 (sh), 1195 (m), 1160 (m), 1090 (sh), 1030 (s), 1010 (sh), 1000 (sh), 980 (s), 910 (m), 835 (m), 750 (sh), 730 (sh), 720 (sh), 710 (sh), 615 (w), 580 (m).

X-ray crystallography. Complex 4. Data were collected at a temperature of −160 °C using the ω-2θ scan technique to a maximum 2θ value of 50.0° for a suitable air-sensitive crystal mounted on a glass fiber. Cell constants and orientation matrix were obtained from the least-squares refinement of 23 carefully centered reflections in the range $46.24° < 2\theta < 49.11°$ corresponding to a triclinic cell. Of the 4400 reflections which were collected, 4134 were unique. The intensities of three representative reflections were measured after every 150 reflections indicating crystal and electronic stability. Data were corrected for Lorentz and polarization effects but not for absorption. The structure was solved by direct methods. The non-hydrogen atoms were refined anisotropically. Hydrogen atom positions were located in the difference Fourier maps but not refined. The final cycle of full-matrix least-squares refinement was based on 3475 observed reflections [$I > 2.5\sigma(I)$] and 365 parameters. Neutral atomic scattering factors were taken from Cromer and Waber.[15] Anomalous dispersion effects were included in F_c. All calculations were performed using the TEXSAN package on a Digital VAX station. Details on data collection and structure refinement are reported in Table I. The final atomic coordinates are given as supplementary material. Selected bond distances and angles are given in Table II.

Complex 5. A suitable air-sensitive crystal was sealed in a thin-walled glass capillary and mounted at room temperature on an Enraf-Nonius CAD-4F diffractometer. Unit cell parameters and their standard deviations were derived from setting angles of 25 reflections in the range $35° < 2\theta < 45°$. The intensity of three reference reflections measured every 3 h of X-ray exposure time gave no indication of crystal decomposition. The net intensities of the data were corrected for the scale variation and Lorentz and polarization effects but not for absorption. Standard deviations obtained from counting statistics were increased according to an analysis of the excess variance of the three reference reflections. The structure was solved by Patterson methods and subsequent partial structure expansion by using the NRCVAX structure solution and refinement. The positional and anisotropic thermal parameters for the non-hydrogen atoms were refined with block-diagonal least-squares procedures. The hydrogen atoms were included at their calculated positions in the final refinement riding on their carrier atoms. Weights were introduced in the final refinement cycles. Final refinement on F was carried out by full-matrix least-squares with anisotropic thermal parameters for the non-hydrogen atoms and one overall temperature factor for the hydrogen atoms. Details on data collection and structure refinement are reported in Table I. The final atomic coordinates are given as supplementary materials. Selected bond distances and angles are given in Table II. Scattering factors[16] and anomalous dispersion factors[17] were included in F_c.

Complex 6. Data were collected at room temperature using the ω–2θ scan technique to a maximum 2θ value of 47.1° for a suitable air-sensitive crystal sealed in a glass capillary. Cell constants and the orientation matrix were obtained from the least-squares refinement of 24 carefully centered reflections in the range $20.26° < 2\theta < 26.17°$ corresponding to the monoclinic cell. Of the 3301 reflections which were collected, 3182 were unique. The intensities of three representative reflections were

---

[15] Cromer, D. T.; Waber, J. T. *International Tables for X-ray Crystallography*; The Kynoch Press: Birmingham, England, 1974; Vol. IV.

[16] Cromer, D. T.; Mann, J. B. *Acta Crystallogr.* **1968**, *A24*, 321.

[17] Cromer, D. T.; Liberman, D. J. *J. Chem. Phys.* **1970**, *53*, 1891.

Table I. Crystal Data and Structural Analysis Results

complex	4	5	6	7	14
formula	$C_{54}H_{72}O_2N_2V$	$C_{42}H_{42}O_2N_2V$	$C_{51}H_{41}O_2N_3V$	$C_{20}H_{30}O_4N_2V$	$C_{39}H_{45}O_{10}V_2N_2Si$
fw	832.12	657.74	778.85	413.41	831.76
cryst system	triclinic	monoclinic	monoclinic	orthorhombic	triclinic
space group	$P\bar{1}$	$P2_1/a$	$C2/c$	$Pna2_1$	$P\bar{1}$
a (Å)	9.701(2)	16.373(1)	20.65(2)	13.519(5)	14.443(6)
b	15.303(3)	11.1624(9)	14.28(1)	13.856(4)	15.039(6)
c (Å)	9.000(2)	19.536(3)	16.08(1)	11.196(2)	10.679(3)
α (deg)	101.99(2)				100.66(3)
β (deg)	112.59(2)	97.35(1)	119.89(7)		97.46(3)
γ (deg)	74.20(2)				113.84(3)
V (Å^3)	1179.0(4)	3541.3(7)	4113(7)	2096(1)	2030(1)
Z	1	4	4	4	2
radiation λ (Mo Kα) (Å)	0.710 69	0.710 69	0.710 69	0.710 69	0.710 69
T (°C)	−158	25	25	−158	−162
D_{calcd} (g cm^{-3})	1.172	1.234	1.258	1.310	1.360
μ_{calcd} (cm^{-1})	2.42	5.7	2.74	4.82	5.28
R_F, R_w	0.053, 0.068	0.044, 0.017	0.053, 0.049	0.037, 0.047	0.045, 0.060

Table II. Selected Bond Distances (Å) and Angles (deg)

4	5	6	7	14
V(1)–O(1) = 1.916(2)	V(1)–O(1) = 2.000(3)	V(1)–N(1) = 2.103(8)	V(1)–O(1) = 2.068(4)	V2–V2a = 2.498(1)
V(1)–N(1) = 2.235(2)	V(1)–O(2) = 2.038(3)	V(1)–N(2) = 2.198(5)	V(1)–O(2) = 2.105(3)	V2–N1 = 1.847(3)
O(1)–C(6) = 1.351(3)	V(1)–N(1) = 2.256(3)	V(1)–O(1) = 2.025(4)	V(1)–O(3) = 2.172(4)	N1–N2 = 1.377(4)
O(1)–V(1)–N(1) = 93.39(8)	V(1)–N(2) = 2.202(4)	N(1)–V(1)–N(2) = 94.7(1)	V(1)–O(4) = 2.163(4)	V2–O7 = 1.894(3)
N(1)–V(1)–N(1a) = 180.00	O(1)–V(1)–O(2) = 173.41(13)	N(1)–V(1)–O(1) = 101.9(1)	V(1)–N(1) = 2.245(4)	V2–O8 = 2.264(2)
O(1)–V(1)–O(1a) = 180.00	O(1)–V(1)–N(1) = 92.23(15)	O(1)–V(1)–O(1a) = 156.3(2)	V(1)–N(2) = 2.208(4)	V1–O3 = 2.177(2)
	O(1)–V(1)–N(2) = 95.70(15)	N(2)–V(1)–N(2a) = 170.5(3)	O(1)–V(1)–O(3) = 95.1(1)	V1–O4 = 1.920(2)
	N(1)–V(1)–N(2) = 82.41(13)	O(1)–V(1)–N(2) = 93.0(2)	O(1)–V(1)–O(2) = 168.7(1)	V1–V1a = 3.089(2)
	V(1)··H(118) = 2.504		O(1)–V(1)–O(4) = 77.3(1)	V1–O1 = 1.974(2)
	V(1)··H(218) = 2.544		O(1)–V(1)–N(1) = 97.1(1)	N1–V2–N1a = 94.9(1)
			O(1)–V(1)–N(2) = 94.7(1)	O9–V2–O10 = 75.9(1)
				O7–V2–O8 = 74.90(9)
				O3–V1–O4 = 77.00(9)
				V1–O1–V1a = 102.1(1)
				O1–V1–O1 = 77.8(1)
				N1–N2–C36 = 117.6(3)

measured after every 150 reflections indicating crystal and electronic stability. Data were corrected for Lorentz and polarization effects but not for absorption. The structure was solved by direct methods. The non-hydrogen atoms were refined anisotropically. Hydrogen atom positions were calculated and refined isotropically with one common thermal parameter. The final cycle of full-matrix least-squares refinement was based on 1505 observed reflections [$I > 2.5\sigma(I)$] and 259 parameters. Neutral atomic scattering factors were taken from Cromer and Waber.[15] Anomalous dispersion effects were included in the calculation of the structure factors. All calculations were performed using the TEXSAN package on a Digital VAX station. Details on data collection and structure refinement are reported in Table I. The final atomic coordinates are given as supplementary material. Selected bond distances and angles are given in Table II.

Complex 7. Data were collected at a temperature of −160 °C using the ω–2θ scan technique to a maximum 2θ value of 49.9° for a suitable air-sensitive crystal mounted on a glass fiber. Cell constants and orientation matrix were obtained from the least-squares refinement of 24 carefully centered reflections in the range $30.18° < 2\theta < 42.80°$ corresponding to the orthorhombic cell. Of the 2156 reflections which were collected, 2116 were unique. The intensities of three representative reflections were measured after every 150 reflections indicating crystal and electronic stability. Data were corrected for Lorentz and polarization effects but not for absorption. The structure was solved by direct methods. The non-hydrogen atoms were refined anisotropically. Hydrogen atom positions were calculated and refined isotropicaly with one common thermal parameter. The final cycle of full-matrix least-squares refinement was based on 1669 observed reflections [$I > 2.5\sigma(I)$] and 244 parameters. Neutral atomic scattering factors were taken from Cromer and Waber.[15] Anomalous dispersion effects were included in F_c. All calculations were performed using the TEXSAN package on a Digital VAX station. Details on data collection and structure refinement are reported in Table I. The final atomic coordinates are given as supplementary material. Selected bond distances and angles are given in Table II.

Complex 14. Data were collected at a temperature of −162 °C using the ω–2θ scan technique to a maximum 2θ value of 50.0° for a suitable air-sensitive crystal mounted on a glass fiber. Cell constants and orientation matrix were obtained from the least-squares refinement of 25 carefully centered reflections in the range $37.27° < 2\theta < 46.55°$ corresponding to the triclinic cell. Of the 7255 reflections which were collected, 6946 were unique. The intensities of three representative reflections were measured after every 150 reflections indicating crystal and electronic stability. Data were corrected for Lorentz and polarization effects but not for absorption. The structure was solved by direct methods. The non-hydrogen atoms were refined anisotropically. Hydrogen atom positions were calculated and refined isotropically with one common thermal parameter. The final cycle of full-matrix least-squares refinement was based on 5530 observed reflections [$I > 2.5\sigma(I)$] and 488 parameters. Neutral atomic scattering factors were taken from Cromer and Waber.[15] Anomalous dispersion effects were included in F_c. All calculations were performed using the TEXSAN package on a Digital VAX station. Details on data collection and structure refinement are reported in Table I. The final atomic coordinates are given as supplementary material. Selected bond distances and angles are given in Table II.

Results and Discussion

As illustrated in Schemes I and II, both the structure of V(aryloxide)$_n$ and the final oxidation state of the metal were not determined by the synthetic pathway used for their preparation. The reactions of $[Mz_2V(py)]_2(N_2)$ with ROH [R = 2,6-(t-Bu)$_2$-4-Me-C_6H_2, 2,6-Ph$_2$-C_6H_3, 2-(CH_3O)C_6H_4] proceeded in a similar manner in toluene at low temperature, invariably evolving N_2 and forming the final compound which could be isolated in crystalline form. Higher yields (ca. 65%) could be obtained either by treatment of the reaction mixture with a small excess of pyridine or by using $(Mz)_2V(Py)_2$ as a starting material. The reactions of $(TMEDA)_2VCl_2$ with the corresponding sodium phenoxides were carried out in THF at room temperature. Although attempts to isolate TMEDA adducts were unsuccessful in the case of **4**, subsequent treatment of the reaction mixtures with pyridine gave the same product formed by the reactions of complex **1** and **2**. The reactions of $VCl_2(TMEDA)_2$ with sodium aryloxides were

Scheme I

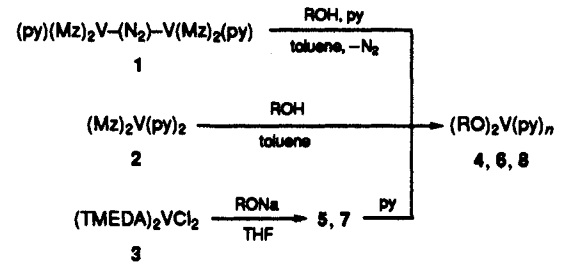

R = 2,6-(t-Bu)$_2$-4-Me-C$_6$H$_2$ (4), 2,6-(Ph)$_2$-C$_6$H$_3$ (5, 6), 2-(CH$_3$O)C$_6$H$_4$ (7,8); Mz = 2-Me$_2$NCH$_2$C$_6$H$_4$; TMEDA = Me$_2$NCH$_2$CH$_2$NMe$_2$; py = pyridine

Scheme II

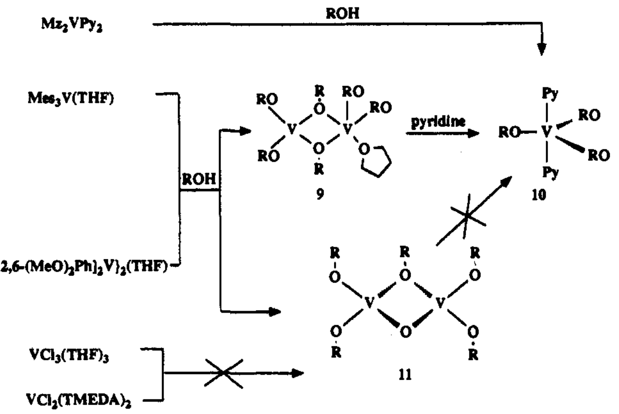

Scheme III

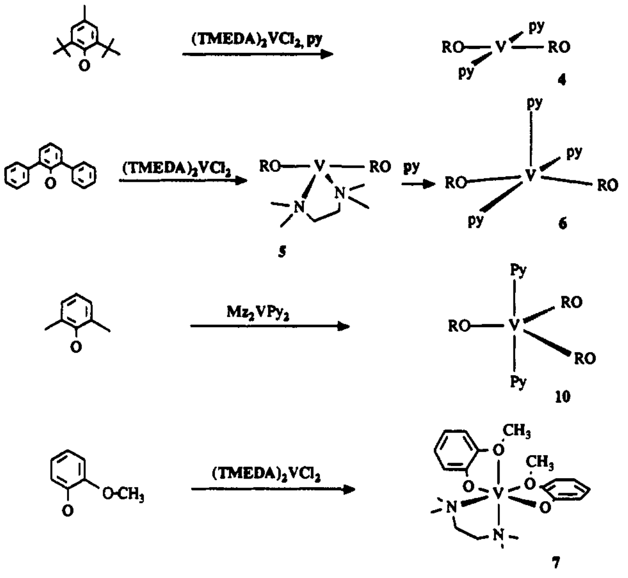

generally slow and, in order to be completed, required several hours of stirring and occasional reflux. For example, during the preparation of **4**, red monoclinic crystals were isolated after 1 h of stirring at room temperature. X-ray analysis[18] revealed a curious co-crystallization phenomenon where the starting VCl$_2$(TMEDA)$_2$ and complex **4** co-crystallized in the same unit cell in a 1:1 ratio. Analytically pure crystals of **4** could be obtained only after 15 h of reflux. Complex **7** was also coveniently prepared via reaction of VCl$_2$(TMEDA)$_2$ with neat guaiacol in the presence of excess of TMEDA.

In contrast, oxidation and formation of V(III) aryloxides was observed when less bulky phenols or aliphatic alcohols (t-BuOH) were employed. In the case of 2,6-Me$_2$PhOH, we have previously described[8a] that the nuclearity (monomeric vs dimeric) and the oxidation state of the metal in the starting complex (II or III) does not affect the result of the reaction, because both dimeric and monomeric V(III) species V(OR)$_3$L$_n$ [R = 2,6-Me$_2$Ph; L = THF (**9**), py (**10**)] have been obtained, depending on the coordinating ability of the Lewis base (Scheme II). Complex **10** was also formed from starting materials **1** and **2** upon reaction with 2 equiv of phenol. When similar reactions were carried out using t-BuOH, another oxidation reaction took place forming the mixed-valence V(III)/V(IV) dimeric species [(t-BuO)$_2$V]$_2$(μ-O)[μ-O(t-Bu)].[19] In this case, we have found no evidence that cleavage of the dinuclear frame might occur upon treatment with a Lewis base (THF, pyridine). Complex **11** also could not be prepared from VCl$_3$(THF)$_3$ or VCl$_2$(TMEDA)$_2$ with (t-BuO)M [M = Li, Na, K], since the reactions led to the formation of pink-purplish hexane-insoluble microcrystalline products, probably metalates. The reaction of **2** with t-BuOH also gave poorly-defined deep-orange products. The magnetic moment of **11** (μ_{eff} = 2.71 μ_B) is significantly lower than expected for a V(III)/V(IV) mixed-valence species and suggests some extent of electronic coupling between the two metal centers [V··V = 3.073 Å].

Attempts to prevent these unexplained oxidations by carrying out the reactions at low temperature did not modify the result. The oxidation of the metal and the metal-promoted deoxygenation of the alkoxide during ligand replacement reaction by aryloxides have a few precedents in the literature of other transition metal alkoxides including Cr,[20] and Ti.[22] While both the mechanism and the complete product distribution still need to be clarified, the puzzling structure of the mixed-valence **11**[19] suggests that metal-assisted deoxygenation pathways are most likely responsible. The results summarized in Scheme III clearly indicate that the oxidation state of the final product is determined to a significant extent by the steric shape of the alkoxide organic moiety, since only in the case of sterically demanding or chelating phenols was it possible to preserve the original oxidation state (+II). In the case of the simple phenol, a green crystalline product was obtained from the reaction of VCl$_2$(TMEDA)$_2$ with PhONa, the magnetic moment and analytical data of which suggested a V(III) formulation. The magnetic properties of the V(II) aryloxides reported in this work are generally consistent with a d^3 high-spin electronic configuration in all cases (ranging between 3.53 and 3.83 μ_B) and did not show any apparent relationship with the different coordination numbers and geometries.

The fact that dinitrogen is invariably released from the V–N$_2$–V frame of **1** during the formation of both V(II) and V(III) aryloxides indicates an intrinsic inability of oxygen donor atom to stabilize dinitrogen complexes. This is in striking contrast to the catalytic features displayed by *in situ* generated V(II) hydroxide and catecholate.[5] Having now available the first series of V(II) aryloxides, we investigated the reactivity of V(II) aryloxides with diazoalkanes, which, having a N–N multiple bond, posses a structure and electronic configuration somewhat reminiscent of a dinitrogen molecule that has been alkylated and reduced by two electrons. The reaction of **7** with (Me$_3$Si)CHN$_2$ was rather slow at room temperature, requiring at least 24 h to complete (Scheme IV) and did not show appreciable gas evolution during the reaction time. Black crystals of the diamagnetic and

---

[18] C$_{52}$H$_{88}$O$_2$N$_6$Cl$_2$V$_2$, *M* = 1002.09, monoclinic, *P*2$_1$/*a*, *a* = 11.204(4) Å, *b* = 14.431(4) Å, *c* = 17.703(6) Å, *V* = 2764.7(15) Å^3, *Z* = 2, λ = 0.710 69 Å, *R* = 0.056, *R*$_w$ = 0.033, and GoF = 2.27, for 445 parameters and 2735 out of 4834 unique reflections.

[19] C$_{20}$H$_{45}$O$_6$V$_2$, *M* = 438.46, orthorhombic, *C*222$_1$, *a* 12.712(3) Å, *b* = 15.234(2) Å, *c* = 17.829(3) Å, *V* = 3453(6) Å^3, *Z* = 4, λ = 0.710 69 Å, *R* = 0.13, and *R*$_w$ = 0.16, for 70 parameters and 616 out of 1493 unique reflections.

[20] Edema, J. J. H.; Gambarotta, S.; Smeets, W. J. J.; Spek, A. L. *Inorg. Chem.* **1991**, *30*, 1380.

[21] Evans, W. J.; Sollberger, M. S.; Shreeve, J. L.; Olofson, J. M.; Hain, J. H.; Ziller, J. W. *Inorg. Chem.* **1992**, *31*, 2492.

[22] Duchateau, R.; Minhas, R.; Gambarotta, S.; Bensimon, C. *Inorg. Chem.* **1992**, *31*, 4933.

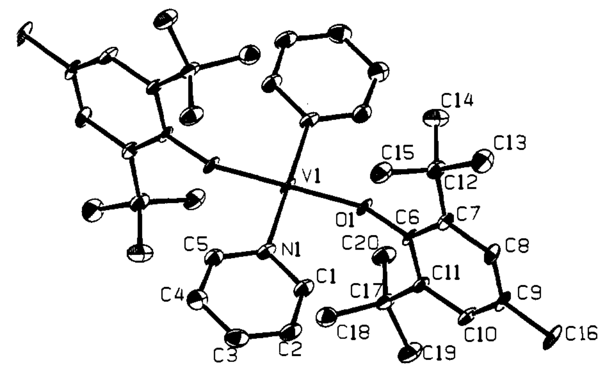

Figure 1. ORTEP plot of **4**. Thermal ellipsoids are drawn at the 50% probability level.

Scheme IV

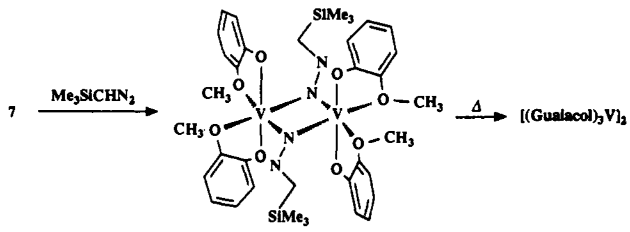

dimeric $\{2\text{-}(CH_3O)C_6H_4]_2V\}_2[\mu\text{-}NN{=}CH(SiMe_3)]_2$ (**13**) were isolated from toluene/hexane mixtures. Complex **13** is thermally unstable in boiling toluene, rapidly decomposing into a complicated mixture where the $\{[2\text{-}CH_3O)C_6H_4O]_3V\}_2$ dimer was the only clearly identifiable product (Scheme IV). Although attempts to grow crystals suitable for X-ray analysis failed, complex **13** co-crystallized very conveniently with $\{[2\text{-}(CH_3O)C_6H_4O]_3V\}_2$ in a 1/1 ratio forming well-formed black-brown cubes of the co-crystallite $\{2\text{-}(CH_3O)C_6H_4]_2V[\mu\text{-}NN{=}CH(SiMe_3)]\}_2/\{[2\text{-}(CH_3O)C_6H_4O]_3V\}_2$ (**14**). An X-ray crystal structure determination has thus demonstrated the structures of both compounds. The diamagnetism of **13** together with the remarkably short V–V distance [V2–V2a = 2.498(1) Å], as determined in the solid-state structure, indicate a significant extent of direct V–V bonding between the two V(IV) atoms. Furthermore, the sharpness of the peaks of the well-solved ^{1}H-NMR spectrum of **13** indicate that the dinuclear structure is retained in solution of hydrocarbon solvents. However, due to the fact that the dinuclear frame can be easily cleaved via coordination of a Lewis base (pyridine)[23] and that a V–V distance as short as 2.4 Å has been demonstrated to be nonbonding,[24] we suggest that the intermetallic contact may be just the result of optimization of bond distances and angles as determined by the two bridging nitrogen atoms of the two diazo moieties. In other words, the short V–V distance should be regarded as a ligand artifact in spite of the fact that it is indeed one of the shortest ever found among dinuclear compounds of tetravalent vanadium.[25]

X-ray Crystal Structures. The structure of **4** shows the molecule having a perfect square-planar geometry around the vanadium atom [N1–V–O1 = 90.0(2)°], with the two aryloxide ligands placed in *trans* positions (Figure 1). The V–O distance [V–O1 = 1.901(8) Å] is slightly shorter than those observed in other V(II)[4] and V(III)[8] alkoxides. The angle formed by the oxygen atom is considerably flattened [V–O1–C4 = 167.8(4)°], probably as a result of both large steric congestion and partial V–O π-bond character. In agreement with these considerations, the V–N distance [V–N1 = 2.240(10) Å] is longer than in $VCl_2(py)_4$[26] and compares well with that found in the sterically encumbered $(Mz)_2V(py)_2$.[10] The square-planar arrangement, similar to that observed in the monomeric anionic $(DIPP)_4VLi_2$ [DIPP = $2,6\text{-}(i\text{-}Pr)_2C_6H_3O$],[4a] is one of the rare cases encountered in the chemistry of vanadium.

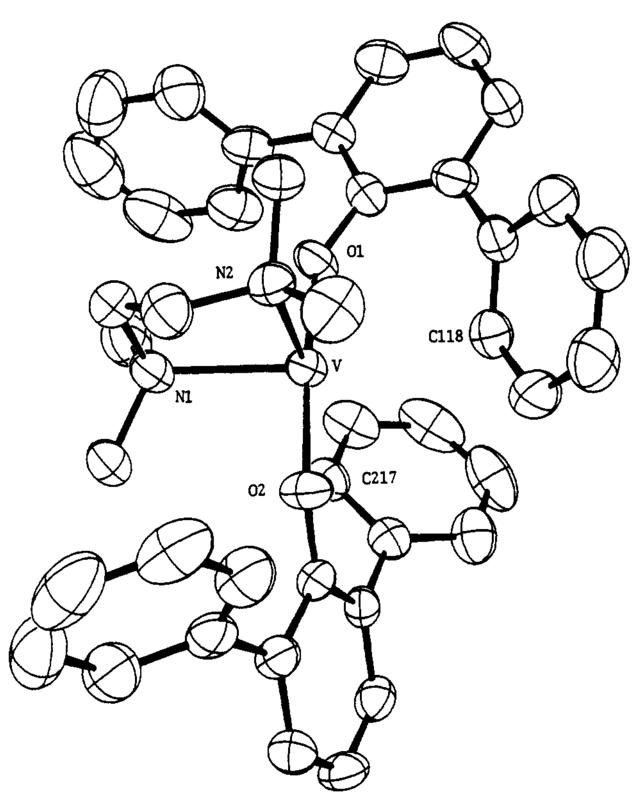

Figure 2. ORTEP plot of **5**. Thermal ellipsoids are drawn at the 50% probability level.

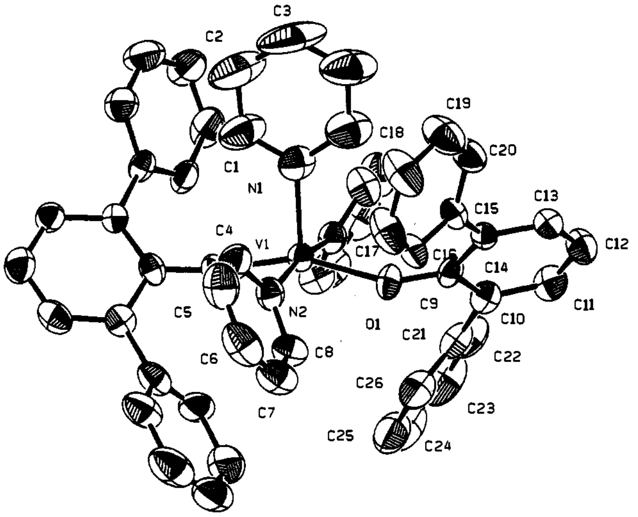

Figure 3. ORTEP plot of **6**. Thermal ellipsoids are drawn at the 50% probability level.

The structure of **5** showed a very unusual saddle-shaped coordination geometry of the vanadium atom (Figure 2) with the two oxygens of the two aryloxide groups almost aligned with the metal [O1–V–O2 = 173.4(1)°]. Conversely the angle formed by vanadium with the two nitrogen atoms of the TMEDA molecule is rather narrow [N1–V–N2 = 82.4(1)°]. The V–O and V–N distances are normal (Table II) and compare well with those of other V(II) aryloxides[4,8] and TMEDA derivatives.[10,27] Considerably short V··H nonbonding distances [V··H(118) = 2.544 Å;

---

[23] Minhas, R.; Hao, S.; Gambarotta, S. Manuscript in preparation.

[24] Poumbga, C.; Daniel, C.; Benard, M. *Inorg. Chem.* **1990**, *29*, 2387.

[25] (a) Duraj, S. A.; Andras, M. T.; Kibala, P. A. *Inorg. Chem.* **1990**, *29*, 1232. (b) Reynolds, J. C.; Sendlinger, S. C.; Murray, A. M.; Huffman, J. C.; Gristhou, G. *Angew. Chem., Int. Ed. Engl.* **1992**, *31*, 1753. (c) Ruiz, J.; Vivanco, M.; Floriani, C.; Chiesi-Villa, A.; Guastini, C. *J. Chem. Soc., Chem. Commun.* **1991**, *214*.

[26] Brauer, D. J.; Kruger, C. *Cryst. Struct. Commun.* **1973**, *3*, 421.

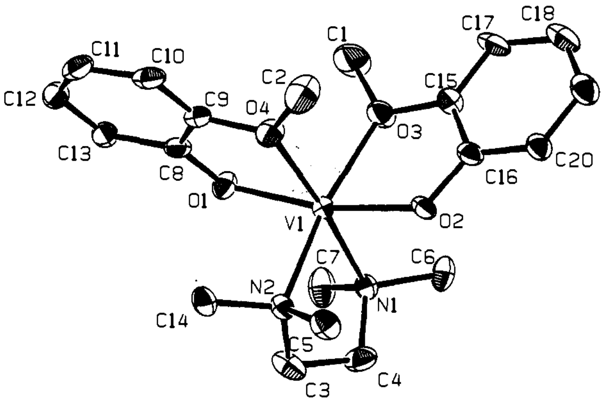

Figure 4. ORTEP plot of **7**. Thermal ellipsoids are drawn at the 50% probability level.

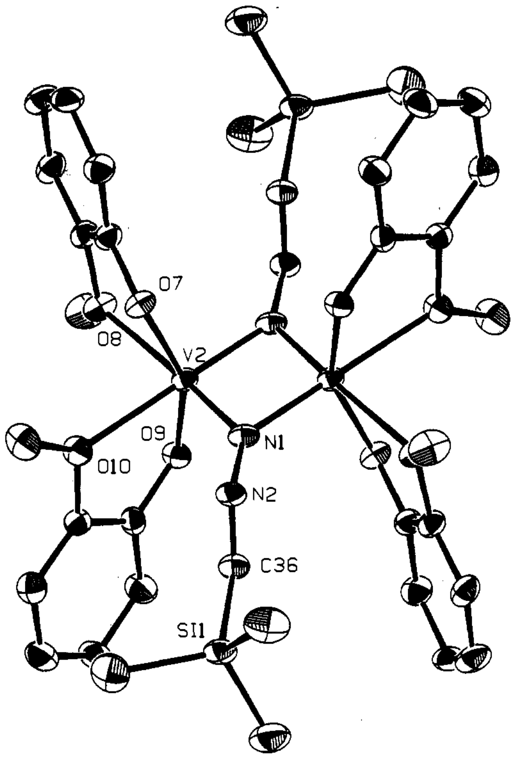

Figure 5. ORTEP plot of **14** (first molecule). Thermal ellipsoids are drawn at the 50% probability level.

V··H(218) = 2.5436 Å] are formed by the vanadium atom with two hydrogen atoms each placed in one of the two *ortho* position of one of the two phenyl rings of each aryloxide ligand. If we consider this double-agostic interaction as real, the molecule may be also regarded as formed by a vanadium atom placed in the center of a rather regular octahedron with the two oxygen atoms occupying the two apical *trans* positions, the TMEDA nitrogen atoms on the two *cis* equatorial positions, and the last two equatorial positions occupied by the two agostic hydrogen atoms. Although the V··H distances are rather short, we believe that these interatomic contacts are probably artifacts of the particular geometry of the bulky aryloxide groups and therefore unlikely to be able to contribute to the stabilization of the metal center.

The structure of complex **6** showed the vanadium atom possessing a rare square-pyramidal geometry[28] (Figure 3). Two molecules of pyridine and the two oxygen atoms of two alkoxides define the basal plane forming V–O and V–N distances [V1–O1 = 2.025(4) Å; V1–N1 = 2.103(8) Å; V1–N2 = 2.198(5) Å] which compare well with those of the other compounds reported in this work. The angle formed by vanadium with the two oxygen atoms [O1–V1–O1a = 156.3(2)°] is significantly narrower than in complex **5** suggesting that in this case the geometry can be considered somewhere between a square pyramidal and trigonal bipyramidal. The two basal pyridine molecules are almost linearly placed in *trans* to each other with respect to the metal [N2–V–N2a = 170.5(3)°]. Differently from the case of the closely related (pyrrolyl)$_2$Cr(py)$_3$,[29] no significant differences have been found in the V–N bond distances formed with the metal by the equatorial and axial pyridine.

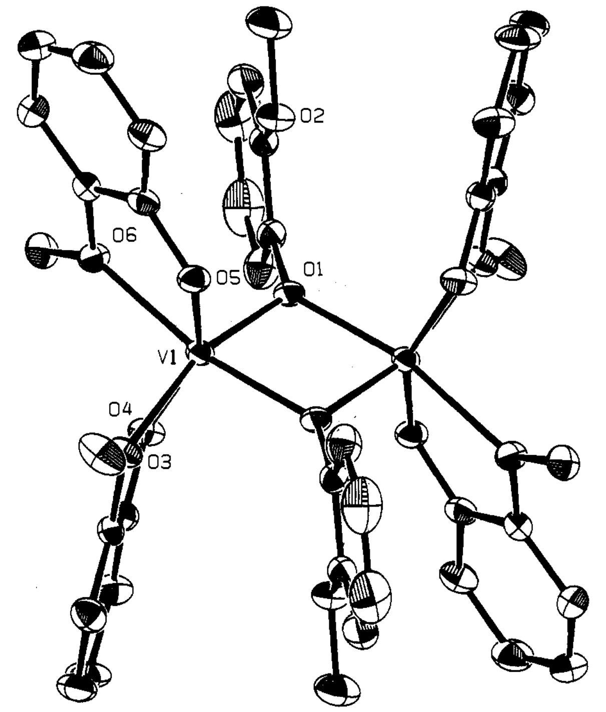

Figure 6. ORTEP plot of **14** (second molecule). Thermal ellipsoids are drawn at the 50% probability level.

The structure of complex **7** has shown an hexacoordinated vanadium atom placed in the center of a slightly distorted octahedral structure (Figure 4). The coordination octahedron is defined by four oxygen atoms of two guaiacol moieties and two nitrogen of TMEDA. The angles formed by vanadium with the three chelating ligands [O1–V–O4 = 77.3(1)°; O2–V–O3 = 76.0(1)°; N1–V–N2 = 82.0(2)°] are similar and impose an overall propeller-shape of the complex. The V–O and V–N distances [V–O1 = 2.068(4) Å; V–O4 = 2.163(4) Å; V–N1 = 2.245(4) Å] are as expected.

The structure of the co-crystallite **14** is composed of two independent [2-(CH$_3$O)C$_6$H$_4$O]$_3$V}$_2$[μ-NN=CH(SiMe$_3$)]$_2$ and [2-(CH$_3$O)C$_6$H$_4$O]$_3$V}$_2$ molecules. The dimeric structure of the first unit is made by two (Guaiacol)$_2$V moieties bridged by the terminal nitrogen atoms of two bridging (Me$_3$Si)CHN$_2$ groups (Figure 5). The V$_2$N$_2$ core is planar (torsion angle V2–N1–N1a–V2a = 0.00°) and is characterized by a short V–V distance [V2–V2a = 2.498(1) Å]. The angle formed by the bridging nitrogen with the two vanadium atoms [V2–N1–V2a = 85.1(1)°] deviates significantly from that expected for an sp^2 nitrogen atom. The V–N distance is rather short [V2–N1 = 1.847(3) Å] and together with the trigonal planar geometry of the bridging atom suggests some extent of π-bonding with the two metals. In agreement with these considerations, the N–N distance of the diazo moiety [N1–N2 = 1.377(4) Å] is only slightly shorter than

---

(27) Edema, J. J. H.; Metsma, A.; vanBolhuis, F.; Gambarotta, S. *Inorg. Chem.* **1991**, *30*, 2056.

(28) Edema, J. J. H.; Gambarotta, S.; Meetsma, A.; Spek, A. L.; Veldman, N. *Inorg. Chem.* **1991**, *30*, 2062.

(29) Edema, J. J. H.; Gambarotta, S.; Meetsma, A. vanBolhuis, F.; Spek, A. L.; Smeets, W. J. J. *Inorg. Chem.* **1990**, *29*, 2147.

expected for a N–N single bond.[30] In agreement with a significant degree of N–N double-bond reduction, the N–N–C array is bent [N1–N2–C36 = 117.6(3)°]. The (Guaiacol)$_2$V unit is normal with the expected V–O bond distances and angles [V2-O7 = 1.894(3) Å; V2–O8 = 2.264(2) Å] which compare well with those of complex **7**. The coordination geometry of vanadium is distorted octahedral [N1–V2–N1a = 94.9(1)°; O9–V2–O10 = 75.9(1)°; O7–V2–O8 = 74.90(9)°]. The second molecule cocrystallized with **13** is also dimeric and is similarly composed by two (Guaiacol)$_2$V units [V1–O3 = 2.177(2) Å; V1–O4 = 1.920(2) Å; O3–V1–O4 = 77.00(9)°] bridged by two oxygen atoms of two guaiacols (Figure 6). Apart from the significant differences in the dimetallic core [V1–V1a = 3.089(2) Å; V1–O1 = 1.974(2) Å; V1–O1–V1a = 102.1(1)°; O1–V1–O1 = 77.8(1)°], the bond distances and angles of the (guaiacol)$_2$V fragment compare well with those of complex **13**.

Acknowledgment. This work was supported by the Natural Sciences and Engineering Research Council of Canada (operating grant) and the Petroleum Research Fund, administered by the American Chemical Society. The Nederlandse Organisatie voor Wetenschapeljik Onderzoek (NWO) is gratefully acknowledged for providing a visiting scholarship (J.J.H.E.). We are indebted to Prof. D. Richeson (U. of Ottawa) for helpful discussions.

Supplementary Material Available: Tables listing atomic positional parameters, temperature factors, torsion angles, bond angles and distances, and hydrogen atom positional parameters associated with complexes **4**, **5**, **6**, **7**, and **14** (91 pages); tables of structure factors for the same compounds (109 pages). Ordering information is given on any current masthead page.

---

[30] Frizuk, M. D.; Haddad, T. S.; Rettig, S. J. *J. Am. Chem. Soc.* **1990**, *112*, 8185 and references cited therein.